

Establishment of a patient-derived mucoepidermoid carcinoma cell line with the *CRTC1-MAML2* fusion gene

KAZUMA NOGUCHI^{1*}, SHUJI KANDA^{1*}, KAZUNARI YOSHIDA¹, YUSUKE FUNAOKA¹, KOJI YAMANEGI², KYOHEI YOSHIKAWA¹, KAZUKI TAKAOKA¹, HIROMITSU KISHIMOTO¹ and YOSHIRO NAKANO³

Departments of ¹Oral and Maxillofacial Surgery, ²Pathology and ³Genetics,
Hyogo College of Medicine, Nishinomiya, Hyogo 663-8501, Japan

Received November 29, 2019; Accepted October 8, 2021

DOI: 10.3892/mco.2022.2508

Abstract. Mucoepidermoid carcinoma (MEC) is the most common malignant tumor of the major and minor salivary glands. Surgical resection is the only curative treatment and there is no effective post-operative therapy for MEC. The present study reports an Institutional Review Board-approved case of a 45-year-old Japanese female diagnosed with low-grade MEC in the hard palate. Radical resection, supraomohyoid neck dissection and antero-lateral thigh flap reconstruction was performed. A MEC cell line was then established from the resected tumor tissue. Short tandem repeat profiling confirmed the origin and authenticity of the cell line, that harbors a *CRTC1-MAML2* translocation, which is frequently observed in MEC. Amphiregulin (AREG), identified as one of the targets of the *CRTC1-MAML2* fusion gene, was expressed in the cell line. The AREG receptor, epidermal growth factor receptor (EGFR) was also highly phosphorylated. The results predicted that AREG-EGFR signaling, which is required for tumor growth and survival, might be activated in the cell line in a cell-autonomous manner. As AREG expression is associated with EGFR-targeted drug resistance, this cell line might assist with the identification of novel strategies for MEC treatment.

Introduction

Mucoepidermoid carcinoma (MEC), representing 5% of all salivary gland tumors and 26% of malignant salivary gland

tumors registered for the last 39 years in Hiroshima, Japan, is the most common malignant tumor of the major and minor salivary glands (1,2). MEC is characterized by its cellular heterogeneity and consists of mucin-producing, epidermoid and intermediate cells. Clinical and pathological parameters (age, tumor size, presence of cervical lymphadenopathy, distant spread, perineural invasion and histological grade) of MEC have been associated with tumor biological behavior and patient management (3). Pathological classification of MEC is graded as low-, intermediate- or high-grade based on adverse features, such as perineural invasion, angiolymphatic invasion, coagulative necrosis, infiltrative growth, high mitotic rate, anaplasia and cystic components of <20% (4).

An important genetic abnormality in MEC is the translocation between chromosomes 11q and 19p, which has been hypothesized to be an early event in the pathogenesis of MEC (5,6), and has been reported in >50% of MEC tumors (7). Low-grade tumors have a higher incidence rate of this fusion compared with that in high-grade tumors (8) and patients with fusion-positive cancer tend to have improved survival time, with significantly lower risks of recurrence, metastases or cancer-related mortality (9). The majority of fusion genes in MEC are associated with a specific chromosomal t(11;19)(q14-21;p12-13) translocation that joins exon 1 of the cAMP response element-binding (CREB) protein-binding domain of CREB-regulated transcription coactivator 1 (*CRTC1*) gene to exons 2-5 of the Notch coactivator mastermind-like gene 2 (*MAML2*) gene, resulting in the expression of a new *CRTC1-MAML2* fusion gene (10). This translocation generates a fusion protein comprised of *CRTC1* (also called *MECT1*, *TORC1* or *WAMPI*) at 19q21 and the C-terminal transcriptional activation domain of *MAML2* at 11q21 (11-14). Previous analysis suggested that another member of the *CRTC* family, at 15q26, *CRTC3*, also fused with *MAML2* (15). Okabe *et al* (16) and Nakayama *et al* (17) showed that *CRTC1-MAML2* or *CRTC3-MAML2* fusions occurred in 40-80% of primary salivary gland MECs, and was associated with a distinct tumor subset that had favorable clinicopathological features and an indolent clinical course.

Previously, amphiregulin (AREG), a member of the epidermal growth factor (EGF) family, was identified as a target of the *CRTC1-MAML2* fusion gene and secreted AREG was shown to activate EGF receptor (EGFR) signaling in an

Correspondence to: Dr Kazuma Noguchi, Department of Oral and Maxillofacial Surgery, Hyogo College of Medicine, 1-1 Mukogawa-cho, Nishinomiya, Hyogo 663-8501, Japan
E-mail: knoguchi@hyo-med.ac.jp

*Contributed equally

Abbreviations: MEC, mucoepidermoid carcinoma; AREG, amphiregulin; EGFR, epidermal growth factor receptor

Key words: patient-derived cell line, mucoepidermoid carcinoma, salivary gland carcinomas, *CRTC1-MAML2*, fusion gene

autocrine manner (18). Furthermore, mutations in *EGFR* itself are rare in salivary gland carcinomas (19), while copy number alternations in *EGFR* are frequently found in high-grade MEC, regardless of fusion gene positivity (20). The molecular pathology and oncology of MEC are still poorly understood. Established authentic cell lines are essential to determine the biological characteristics of MEC, and a number of cell cultures and models have emerged; however, the cell line usability is limited (21). The present study reports the establishment of a MEC cell line (HCM-MEC010) carrying the *CRTC1-MAML2* fusion gene and activated *EGFR*. The potential uses for this cell line will also be discussed to understand the biological characteristics of MEC.

Materials and methods

Cell line generation and cell culture. A patient with MEC provided consent in accordance with Hyogo College of Medicine (Hyogo, Japan) institutional policies. Tumor samples were obtained according to an approved Institutional Review Board protocol of Hyogo College of Medicine (approval no. 276; Hyogo, Japan). The present study was also conducted in accordance with the Declaration of Helsinki. Clinical and pathological data were collected from the medical records of the patient. Tumor tissues were minced into 1–2-mm pieces with a disposable scalpel and placed in primary culture. To separate the stromal cells from the mass culture, a magnetic-activated cell sorting (MACS) system was used. Briefly, MACS buffer, containing 1X PBS, 0.5% BSA, 2 mM EDTA (pH 7.2) (cat. no. 130-042-901; Miltenyi Biotec Inc.), was pre-cooled to 4°C. To remove the fibroblasts, the single cell suspension was centrifuged at 300 x g for 10 min at room temperature, and positive selection was performed using CD326 (EpCAM) MicroBeads and a MidiMACSTM Separator (Miltenyi Biotec GmbH), according to the manufacturer's instructions. The obtained primary human MEC cells were seeded in F-medium (22) with 10 µM Y-27632 (FUJIFILM Wako Pure Chemical Corporation). After 1 week, the culture medium was replaced with fresh medium, which was changed every 4 days thereafter. At the same time, the fibroblasts derived from the tumor tissue of the same patient, were obtained and grown in F-medium. Once cells reached confluence (80%), they were washed with PBS (Mg²⁺ and Ca²⁺ free) (23) and detached with 0.05% EDTA/trypsin for 5 min at 38°C (24). After centrifugation at 167 x g for 5 min at 4°C, the MEC cells were resuspended in F-medium, containing Y-27632 and seeded (0.3x10⁶ cells) in 60 mm dishes. An epithelial cell line was successfully established from the sample of the patient and was termed HCM-MEC010. The morphology of the exponentially proliferating cells in a monolayer was reviewed and documented using inverted phase contrast microscopy. The cells were also tested for mycoplasma infection using the MycoAlert® Assay (Lonza Group, Ltd.) and the cell culture growth medium and with fluorescent microscopy using the Mycoplasma Hoechst Stain Assay (MP Biomedicals, LLC).

Short tandem repeat (STR) authentication of the MEC cell line. To verify the identity of the cell line, genomic DNA was extracted from the blood of the patient, whose tumor

sample was used to generate the HCM-MEC010 cell line, as well as from the cell line using the QIAamp DNA Mini kit (Qiagen, Inc.) according to the manufacturer's protocol. DNA genotyping using STR profiling was performed using the GenePrint 10 System (Promega Corporation) and the Applied Biosystems 3130xl Analyzer (Applied Biosystems; Thermo Fisher Scientific, Inc.) and analyzed by BEX Co., Ltd. The evaluation value (EV) was determined using the following equation: EV=(number of coincidental peaks) x 2/total number of peaks in cell A and total number of peaks in cell B.

Reverse transcription (RT)-PCR of the *CRTC1-MAML2* fusion oncogene. The HCM-MEC010 cell line was plated in 100-mm dishes and cultured to 90% confluence. RNA was extracted using TRIzol® (Invitrogen; Thermo Fisher Scientific, Inc.) and RT-PCR was performed using the PrimeScript RT-PCR kit (Takara Bio, Inc.) according to the manufacturer's instructions. The following primers were used: *CRTC1* forward 1, 5'-TTC GAGGAGGTCATGAAGGA-3' and 2, 5'-ATGGCGACT TCGAACAATCCGCGGAA-3'; *MAML2* reverse 1, 5'-TTG CTGTTGGCAGGAGATAG-3' and 2, 5'-GGGTCGCTTGCT GTTGGCAGGAG-3' (18), which amplified 101 and 194 bp fragments, respectively. Amplification of the *GAPDH* gene (forward, 5'-CAATGACCCCTTCATTGACC-3' and reverse, 5'-GACAAGCTTCCCGTTCTCAG-3') was performed as a control. Successfully amplified RT-PCR products of the *CRTC1-MAML2* fusion gene were purified and sequenced (24) using BigDye™ Terminator v3.1 Cycle Sequencing kit (Thermo Fisher Scientific, Inc.) and 2% agarose gel electrophoresis.

Western blot analysis. The culture medium was removed and the cells were washed with PBS (Mg²⁺ and Ca²⁺ free). RIPA buffer was added (cat. no. sc-24948; Santa Cruz, Inc.) and the cells were incubated at 4°C for 60 min, then centrifuged at 12,000 x g for 20 min 4°C. The supernatant was the total cell lysate. Proteins were extracted from the HCM-MEC010 and human tongue squamous cell carcinoma (SAS; purchased from the Japanese Collection of Research Bioresources Cell Bank) cell lines as previously described (25). Protein concentration was measured using a Bradford assay (26) Western blot analysis was performed as previously described (25). The primary and secondary antibodies are listed in Table I. The protein expression ratio, compared with that in SAS cells, was measured using ImageJ v1.53e software (National Institutes of Health). The data are presented as the mean ± SD. The experiment was repeated three times.

Immunofluorescence staining. The cultured HCM-MEC010 and SAS cell lines were fixed in 3.7% formaldehyde for 20 min at room temperature. After permeabilization with 0.2% Triton-X/PBS for 5 min at room temperature, the cells were blocked with 2% (w/v) BSA (Nacalai Tesque, Inc.)/PBS, then washed with PBS (Mg²⁺ and Ca²⁺ free) and incubated with the primary antibodies overnight at 4°C. The cells were washed with PBS (Mg²⁺ and Ca²⁺ free), then incubated with the secondary antibody and Rhodamine phalloidin (Cytoskeleton, Inc.) for 2 h at room temperature. The samples were mounted in Vecta shield containing DAPI (Vector Laboratories). Fluorescent images were captured using a

Table I. Primary and secondary antibodies used for western blot analysis and immunofluorescence.

A, Primary antibodies

Name	Cat. no.	Dilution		Supplier
		Western blot	Immunofluorescence	
Rabbit monoclonal anti-EGFR	4267	1/1000	1/60	CST
Rabbit monoclonal anti-p-EGFR	3777	1/1000		CST
Rabbit monoclonal anti-AKT	4691	1/1000		CST
Rabbit monoclonal anti-p-AKT	4060	1/1000		CST
Rabbit monoclonal anti-AREG	16036-1-AP	1/1000		ProteinTech Group, Inc.
Rabbit monoclonal anti-E-cadherin	3195	1/1000	1/100	CST
Rabbit monoclonal anti-N-cadherin	13116	1/1000	1/100	CST
Rabbit monoclonal anti-vimentin	5741	1/1000	1/100	CST
Rabbit monoclonal anti-tubulin	2148	1/1000		CST
Mouse monoclonal anti-actin	47778	1/1000		

B, Secondary antibodies

Name	Cat. no.	Dilution		Supplier
		Western blot	Immunofluorescence	
Alexa Fluor 488 goat anti-rabbit IgG (H+L)	A-11008		1/400	Molecular Probes; Thermo Fisher Scientific, Inc.
Anti-mouse IgG, HRP-linked	7076	1/1000		CST
Anti-IgG (H+L chain) rabbit pAb-HRP	458	1/10000		Molecular and Biological Laboratories Co., Ltd.
Goat anti-mouse HRP	ab97023	1/1000		Abcam

CST, Cell Signaling Technology, Inc.; p, phosphorylated.

confocal laser-scanning microscope (LSM780; Zeiss AG). The primary and secondary antibodies are listed in Table I.

RNA analysis. RNA-Sequencing (RNA-Seq) libraries were generated using RNA extracted from the HCM-MEC010 cell line, as previously described (27), with the TruSeq Stranded mRNA Library Prep kit for Illumina, Inc., following the manufacturer's instructions, then sequenced on a NovaSeq 6000 System (Illumina, Inc.). The analysis was performed by Takara Bio, Inc.

Hematoxylin and eosin-staining. A section of the hard palate was fixed in 10% formalin solution at room temperature for 24 h and embedded in paraffin. Sections (5- μ m thick) were cut from the paraffin blocks and stained with hematoxylin (0.09%) for 5 min and eosin (0.13%) for 9 min at room temperature according to standard methods (28). The images were captured using a light microscope (BX51; Olympus Corporation).

Patient. A 45-year-old Japanese female noticed spontaneous dull pain and swelling in her hard palate for 1 month and was referred to Hyogo College of Medicine, Nishinomiya, Hyogo, Japan on January, 2019. On examination, diffuse

swelling was observed in the right hard palate. There was no trismus. The surface of the mass was smooth and was soft on palpation (Fig. 1A). Bilateral cervical lymph nodes were palpable, but painless and mobile. Magnetic resonance imaging showed an irregular mass measuring 30x20x18 mm in the right hard palate, and resorption in the nasal septum and posterior wall of the maxillary sinus (Fig. 1B). The clinical diagnosis was a malignant tumor of the hard palate. A biopsy was performed intraorally and the lesion was pathologically diagnosed as low-grade MEC using Armed Forces Institute of Pathology (29).

Results

The patient was admitted to Hyogo College of Medicine, Nishinomiya, Hyogo, Japan and treated by partial resection of the hard palate, supraomohyoid neck dissection and reconstruction using an anterolateral thigh flap under general anesthesia. Hematoxylin and eosin-stained tumor tissue microscopically showed an overlying stratified squamous epithelium, mucous cells and squamous cells that were polygonal-to-ovoid in shape with eosinophilic cytoplasm (Fig. 1C). The mucous cells were cuboidal or goblet-like and tended to line the cysts. The

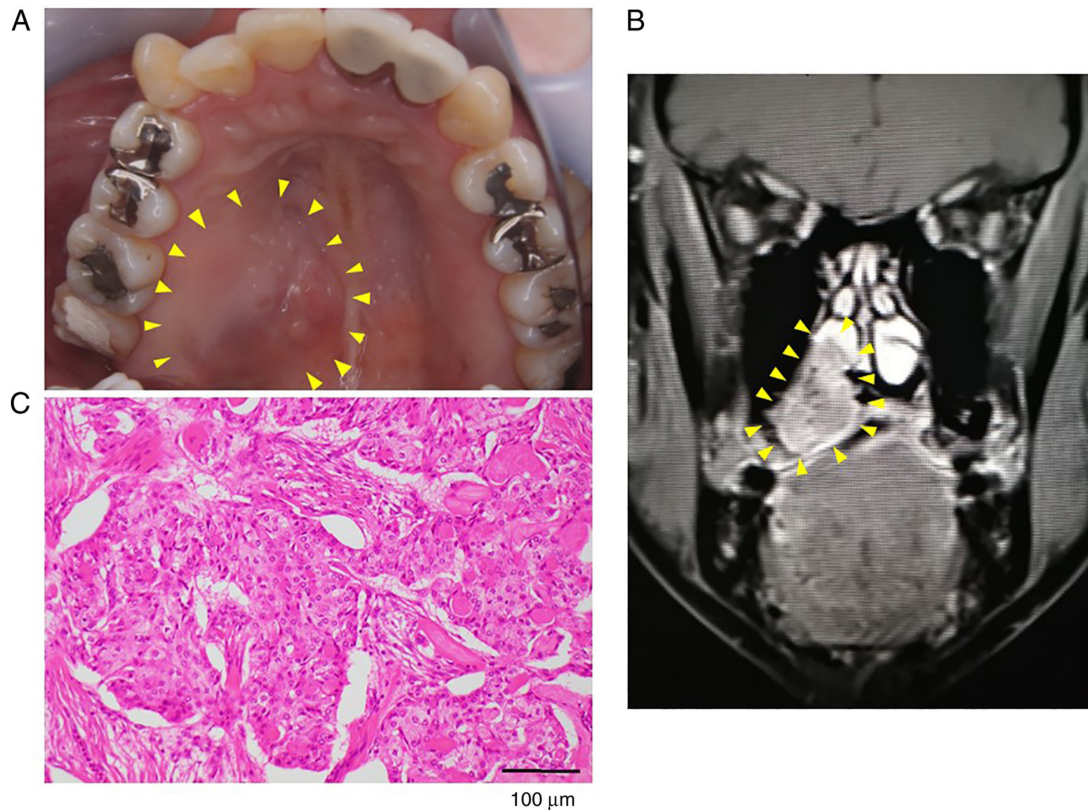


Figure 1. Clinical findings. (A) Normal-colored volumetric tissue with a smooth surface ~30x20 mm in diameter located on the right side of the hard palate (yellow arrowheads). (B) Magnetic resonance imaging showing an irregular mass measuring 30x20x18 mm in the right hard palate and resorption in the nasal septum and posterior wall of the maxillary sinus (yellow arrowheads). (C) Microscopic view showing epidermal cells with very few mucous cells and minimal cystic changes suggestive of mucoepidermoid carcinoma with hematoxylin and eosin staining.

squamous cells formed solid sheets. The tumor was diagnosed as mucoepidermoid carcinoma, low-grade type, pT4aN0M0 MEC of the hard palate. All dissected cervical lymph nodes showed no metastatic cells. At the 30-month follow up, the patient's prognosis was excellent and she had maintained a disease-free status.

Establishment of a MEC cell line from a patient tumor. A new MEC cell line, termed HCM-MEC010 was established, which maintained a cobblestone epithelial-like morphology for at least 30 passages (Fig. 2A and B). To confirm that the HCM-MEC010 cell line was derived from the tumor sample of the patient, STR profiling was performed using the DNA extracted from the high-passage HCM-MEC010 cell line and the blood from the patient. Genotypic analysis confirmed that the cell line was derived from the tumor and no contamination with other cell types was detected (EV, 1.0). (Table S1; Figs. S1 and S2).

RT-PCR analysis reveals that HCM-MEC010 cells express the *CRTC1-MAML2* fusion gene. As the *CRTC1-MAML2* gene fusion is common in MEC (9), the fusion event was analyzed in the HCM-MEC010 cell line using RT-PCR. Fig. 3A shows the translocation event between chromosomes 11 and 19, while Fig. 3B shows the RT-PCR amplified fragments (lane 1, 101 bp and lane 2, 196 bp) using primer sets 1 or 2, respectively. The fusion transcript of *CRTC1* and *MAML2* genes was confirmed using Sanger sequencing (Fig. 3C). This revealed the fusion

products of *CRTC1* exon 1 and *MAML2* exon 2 with the predicted splicing event, indicating that a translocation event had occurred between the first introns of *CRTC1* and *MAML2*.

Protein expression in the HCM-MEC010 cell line. Next, the protein expression of the epithelial and mesenchymal markers in the HCM-MEC010 cell line was confirmed using immunofluorescent staining. EGFR and E-cadherin were expressed on the cell membrane in the HCM-MEC010 cells, while N-cadherin expression was only faintly detected. Vimentin expression was also detected in HCM-MEC010 cells (Fig. 4).

HCM-MEC010 cells express AREG and show EGFR activation. As the AREG-EGFR signaling cascade has been identified as a *CRTC1-MAML2* fusion gene target (18), AREG expression and the status of the EGFR cascade was analyzed in the HCM-MEC010 cell line. The human tongue SAS cell line was used as a comparison as the SAS cell line contains a mutation in the *HER4* gene, which encodes one of the other types of human EGFR, and the authentic *EGFR* pathway is not involved in cell proliferation (30). EGFR was expressed in both cell types, but the AREG expression level was much higher in the HCM-MEC010 cell line compared with that in the SAS cell line (Fig. 5). Furthermore, EGFR was phosphorylated (p) in the HCM-MEC010 cell line compared with that in the SAS cell line, indicating the activation of the EGFR pathway. In addition, the expression level of AKT and p-AKT was lower in the HCM-MEC010 cell line

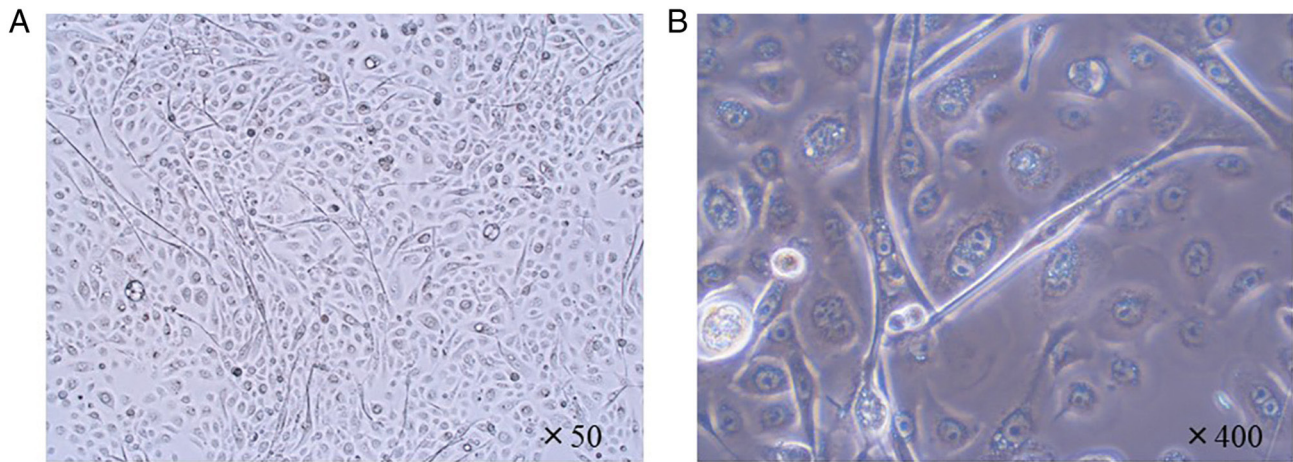


Figure 2. Morphology of the established HCM-MEC010 cells. Microscopic findings of the MEC cell line under (A) low power and (B) high power. MEC, mucoepidermoid carcinoma.

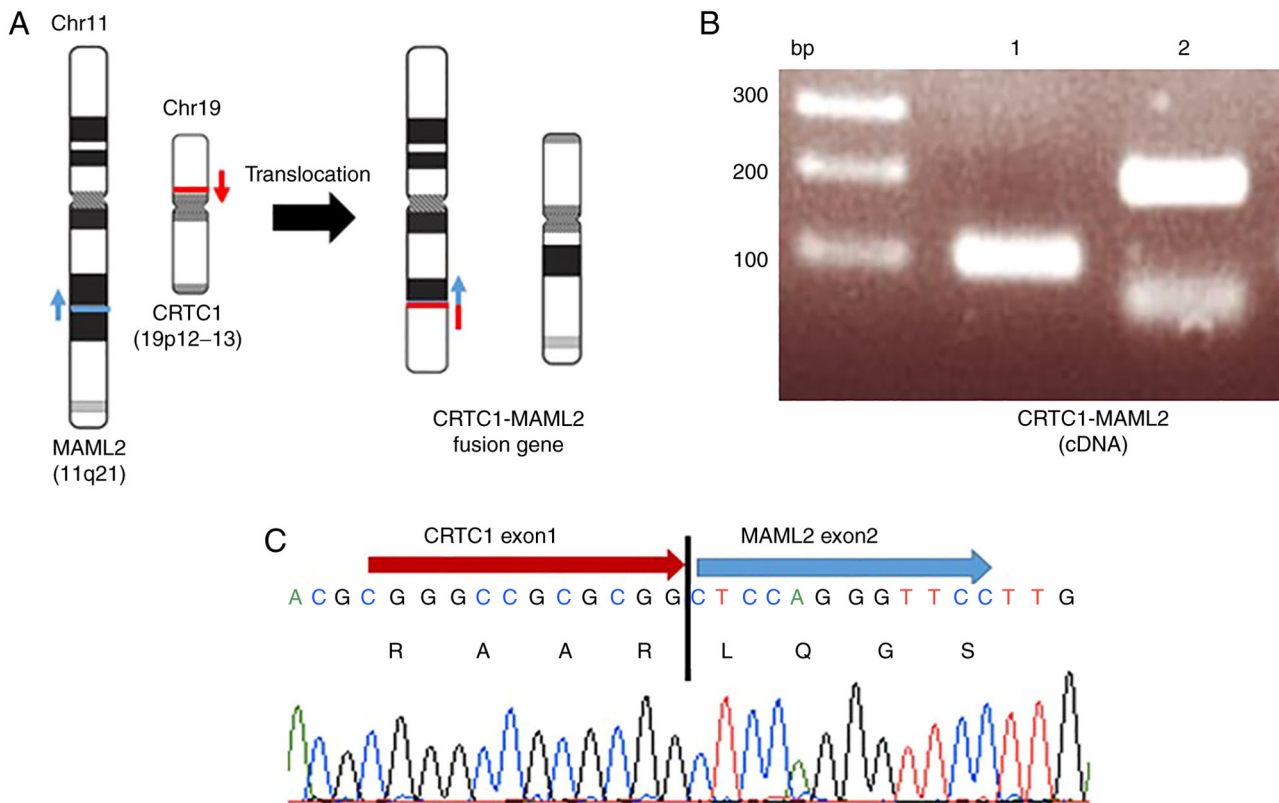


Figure 3. Gene structure of the identified *CRTCI-MAML2* fusion gene. (A) Schematic of *CRTCI-MAML2* gene fusion. (B) Reverse transcription-PCR analysis showing the presence of a *CRTCI-MAML2* fusion transcript. A 101 bp fragment (lane 1) and 194 bp fragment (lane 2) can be seen. (C) Direct sequencing of the *CRTCI-MAML2* fusion gene in the mucoepidermoid carcinoma cell line. *CRTCI*, CREB-regulated transcription coactivator 1; *MAML2*, Notch coactivator mastermind-like gene 2.

compared with that in the SAS cell line. In the SAS cell line, AKT can be phosphorylated by both the AREG-EGFR and HER4 pathways (31,32), and high levels of AKT phosphorylation in the SAS cell line must represent an additive effect of HER4 pathway activation (33). E-cadherin was expressed at higher levels in the HCM-MEC010 cell line compared with that in the SAS cell line. Vimentin expression was detected in small amounts in both the HCM-MEC010 and SAS cell lines (Fig. 5).

RNA-seq analysis of the HCM-MEC010 cell line revealed epidermoid characteristics. To further characterize the HCM-MEC010 cell line, RNA-Seq analysis was performed. MEC is known to be composed of a mixture of mucous, epidermoid, and intermediate cells (34). RNA-Seq analysis revealed the high expression level of genes in the keratin family, including *KRT5*, *KRT14*, *KRT6A*, *KRT17*, and *KRT7*. Table II lists the top 200 expressed genes. However, expression of the mucous cell marker *MUC* was not detected. These

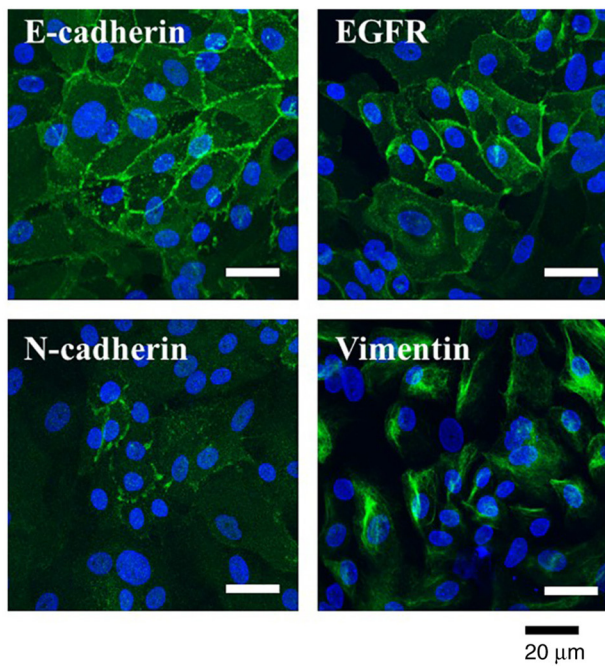


Figure 4. Immunofluorescence staining analysis in the HCM-MEC010 cell line. E-cadherin and EGFR were expressed at high levels. Low expression of N-cadherin and vimentin were observed. EGFR, epidermal growth factor receptor.

results, together with the cell morphology results, suggest that the HCM-MEC010 cell line is considered to be of epidermoid, but not mucinous, origin.

Discussion

The isolation of primary tumor cells from patient samples is the first step for several genetic, biochemical and pharmacological experiments relevant to personalized cancer treatment (35). However, such studies are limited due to cell availability. The establishment of a cancer cell line is a traditional, but still powerful and informative method of studying human cancer. The present study reports the establishment of a MEC cell line with a *CRTC1-MAML2* fusion gene.

Several studies have shown that the presence of the *CRTC1/3-MAML2* fusion gene confers an improved prognosis, with improved disease-free survival and fewer distant metastasis in MEC (36,37). There are rare exceptions to this rule, including fusion-positive high-grade MEC with multiple additional genetic variations, such as mutations in *CDKN2A*, that have been associated with a poor prognosis (38).

The function of the *CRTC1-MAML2* fusion gene has been intensively studied. Its transformation ability was identified using the RK3E cell line (39) and its importance for tumor state maintenance has also been demonstrated. Initially, it was hypothesized to cause tumor growth by the constitutive activation of Notch signaling via the *MAML2* gene portion. Furthermore, the N terminus *CRTC1* domain-mediated aberrant activation of cAMP/CREB signaling has also been identified as a cause of tumor formation (14,40). The interaction between AP-1 and MYC oncoprotein with *CRTC1-MAML2* fusion proteins has been reported (41), suggesting that the *CRTC1-MAML2* fusion gene regulates several different

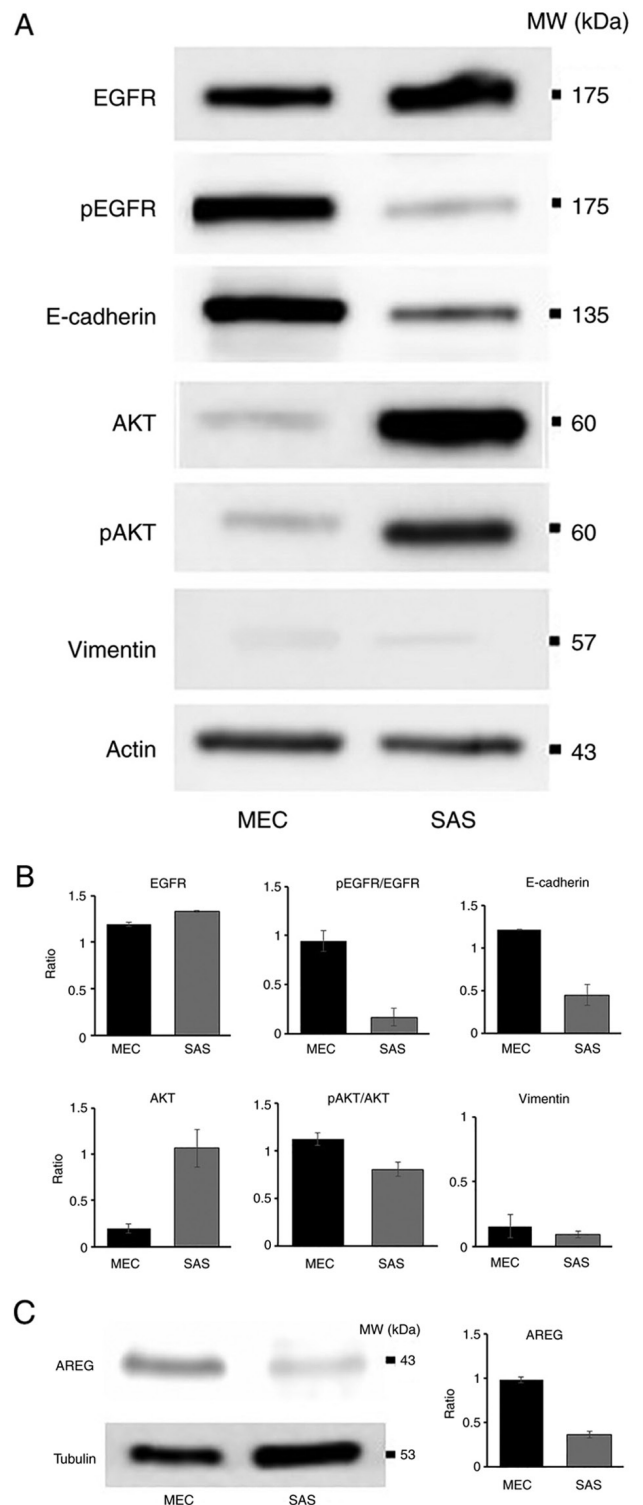


Figure 5. Western blot analysis of EGFR-AKT signaling in the HCM-MEC010 and SAS cell lines. (A) Western blot analysis of EGFR, p-EGFR, E-cadherin, AKT, p-AKT, vimentin and actin and the results were (B) analyzed using densitometry. (C) Western blot analysis of AREG and tubulin. MEC, mucin-epidermoid carcinoma; p, phosphorylated.

signaling pathways. *AREG* is a known cAMP/CREB-regulated gene, whose expression positively correlates with that of *CRTC1-MAML2* in MEC (42). As *AREG-EGFR* signaling was identified as one of the *CRTC1-MAML2* fusion gene targets, *EGFR* signaling could represent the mechanism of action by which the fusion gene promotes carcinogenesis.

Table II. RNA-Sequencing data for the MEC cell line.

Entrez gene ID	Gene symbol	Description	TPM
6280	S100A9	S100 calcium binding protein A9	25012.1582
-	RNR2	-	19355.6582
6277	S100A6	S100 calcium binding protein A6	15991.2832
1915	EEF1A1	Eukaryotic translation elongation factor 1 α 1	13189.91406
9168	TMSB10	Thymosin β 10	11790.02637
3852	KRT5	Keratin 5	10268.93652
6590	SLPI	Secretory leukocyte peptidase inhibitor	9873.083008
6222	RPS18	Ribosomal protein S18	9865.65332
3861	KRT14	Keratin 14	9010.899414
301	ANXA1	Annexin A1	8724.607422
302	ANXA2	Annexin A2	8183.348633
6130	RPL7A	Ribosomal protein l7a	7233.334961
3853	KRT6A	Keratin 6A	7038.019531
6205	RPS11	Ribosomal protein S11	6782.036133
3872	KRT17	Keratin 17	6779
6282	S100A11	S100 calcium binding protein A11	6758.137695
57402	S100A14	S100 calcium binding protein A14	6577.536133
6136	RPL12	Ribosomal protein L12	6571.3125
6202	RPS8	Ribosomal protein S8	5322.165039
23521	RPL13A	Ribosomal protein l13a	5300.688477
6175	RPLP0	Ribosomal protein lateral stalk subunit P0	5200.693848
6144	RPL21 (2)	Ribosomal protein L21	5167.824219
7114	TMSB4X	Thymosin β 4 X-linked	4858.939453
6201	RPS7	Ribosomal protein S7	4807.380371
6281	S100A10	S100 calcium binding protein A10	4705.583984
6206	RPS12	Ribosomal protein S12	4461.196777
6230	RPS25	Ribosomal protein S25	4362.669922
6122	RPL3	Ribosomal protein L3	4190.952148
2597	GAPDH	Glyceraldehyde-3-phosphate dehydrogenase	4084.755371
4502	MT2A	Metallothionein 2A	4024.866699
3855	KRT7	Keratin 7	3954.171631
6194	RPS6	Ribosomal protein S6	3893.395996
6152	RPL24	Ribosomal protein L24	3876.068848
6142	RPL18A	Ribosomal protein l18a	3788.035645
60	ACTB	Actin β	3734.336914
6156	RPL30	Ribosomal protein L30	3719.687988
6279	S100A8	S100 calcium binding protein A8	3664.906982
10399	RACK1	Receptor for activated C kinase 1	3650.605225
100133941	CD24	CD24 molecule	3593.078369
6191	RPS4X	Ribosomal protein S4 X-linked	3478.193848
-	RNR1	-	3421.098877
2950	GSTP1	Glutathione S-transferase pi 1	3338.100586
6187	RPS2	Ribosomal protein S2	3280.663086
6207	RPS13	Ribosomal protein S13	3170.464111
11224	RPL35	Ribosomal protein L35	3153.293701
1937	EEF1G	Eukaryotic translation elongation factor 1 γ	3140.122559
6125	RPL5	Ribosomal protein L5	3137.963623
6170	RPL39	Ribosomal protein L39	3100.071045
4637	MYL6	Myosin light chain 6	3067.146484
3868	KRT16	Keratin 16	3044.359619
4736	RPL10A	Ribosomal protein l10a	2961.195801
6141	RPL18	Ribosomal protein L18	2929.649658

Table II. Continued.

Entrez gene ID	Gene symbol	Description	TPM
1476	CSTB	Cystatin B	2910.897217
6124	RPL4	Ribosomal protein L4	2865.387207
4070	TACSTD2	Tumor associated calcium signal transducer 2	2787.421387
6147	RPL23A	Ribosomal protein l23a	2730.734131
71	ACTG1	Actin γ 1	2705.085693
220	ALDH1A3	Aldehyde dehydrogenase 1 family member A3	2588.035156
6135	RPL11	Ribosomal protein L11	2561.839844
3880	KRT19	Keratin 19	2536.187012
6132	RPL8	Ribosomal protein L8	2522.498047
6181	RPLP2	Ribosomal protein lateral stalk subunit P2	2490.632813
3866	KRT15	Keratin 15	2464.382324
6699	SPRR1B	Small proline rich protein 1B	2444.126465
6159	RPL29	Ribosomal protein L29	2439.016113
2512	FTL	Ferritin light chain	2432.441895
6193	RPS5	Ribosomal protein S5	2432.29126
6233	RPS27A	Ribosomal protein s27a	2403.434326
6129	RPL7	Ribosomal protein L7	2332.271973
6273	S100A2	S100 calcium binding protein A2	2289.59375
6133	RPL9	Ribosomal protein L9	2237.880371
1475	CSTA	Cystatin A	2159.565186
6128	RPL6	Ribosomal protein L6	2119.131592
2495	FTH1	Ferritin heavy chain 1	2094.474121
3921	RPSA	Ribosomal protein SA	2085.400391
5266	PI3	Peptidase inhibitor 3	2079.049805
2171	FABP5	Fatty acid binding protein 5	2073.613281
5052	PRDX1	Peroxiredoxin 1	2053.132568
3956	LGALS1	Galectin 1	2031.178833
6143	RPL19	Ribosomal protein L19	2021.314087
25818	KLK5	Kallikrein related peptidase 5	1822.719238
3939	LDHA	Lactate dehydrogenase A	1803.661499
6176	RPLP1	Ribosomal protein lateral stalk subunit P1	1802.172241
51458	RHCG	Rh family C glycoprotein	1785.147339
6303	SAT1	Spermidine/spermine N1-acetyltransferase 1	1763.299316
9982	FGFBP1	Fibroblast growth factor binding protein 1	1742.557251
7178	TPT1	Tumor protein, translationally-controlled 1	1741.52832
6227	RPS21	Ribosomal protein S21	1726.189087
3934	LCN2	Lipocalin 2	1720.297241
3315	HSPB1	Heat shock protein family B (small) member 1	1668.157104
1973	EIF4A1	Eukaryotic translation initiation factor 4A1	1623.40625
1938	EEF2	Eukaryotic translation elongation factor 2	1612.361694
5055	SERPINB2	Serpin family B member 2	1610.25
2810	SFN	Stratifin	1591.703979
6703	SPRR2D	Small proline rich protein 2D	1568.223389
26986	PABPC1	Poly(A) binding protein cytoplasmic 1	1534.452637
6204	RPS10	Ribosomal protein S10	1532.445679
10410	IFITM3	Interferon induced transmembrane protein 3	1529.12146
6189	RPS3A	Ribosomal protein S3A	1509.361816
6154	RPL26	Ribosomal protein L26	1432.493286
3918	LAMC2	Laminin subunit γ 2	1429.380249
83442	SH3BGL3	SH3 domain binding glutamate rich protein like 3	1395.721313
6139	RPL17	Ribosomal protein L17	1375.231934

Table II. Continued.

Entrez gene ID	Gene symbol	Description	TPM
1933	EEF1B2	Eukaryotic translation elongation factor 1 β 2	1351.424194
10974	ADIRF	Adipogenesis regulatory factor	1348.772461
6134	RPL10	Ribosomal protein L10	1336.026611
5268	SERPINB5	Serpin family B member 5	1335.237183
6700	SPRR2A	Small proline rich protein 2A	1285.784912
10094	ARPC3	Actin related protein 2/3 complex subunit 3	1270.268311
2152	F3	Coagulation factor III, tissue factor	1268.36792
2197	FAU	FAU ubiquitin like and ribosomal protein S30 fusion	1255.56189
9124	PDLIM1	PDZ and LIM domain 1	1252.652954
64065	PERP	P53 apoptosis effector related to PMP22	1252.282227
4869	NPM1	Nucleophosmin 1	1247.643188
7295	TXN	Thioredoxin	1169.833984
3553	IL1B	Interleukin 1 β	1166.45752
5054	SERPINE1	Serpin family E member 1	1154.025146
6171	RPL41	Ribosomal protein L41	1152.395996
25824	PRDX5	Peroxiredoxin 5	1133.30603
6173	RPL36A	Ribosomal protein L36a	1111.359619
5315	PKM	Pyruvate kinase M1/2	1092.81897
1072	CFL1	Cofilin 1	1085.361328
6289	SAA2	Serum amyloid A2	1073.526978
4071	TM4SF1	Transmembrane 4 L six family member 1	1063.068237
506	ATP5F1B	ATP synthase F1 subunit β	1047.457275
5834	PYGB	Glycogen phosphorylase B	1047.218994
928	CD9	CD9 molecule	1021.081299
10628	TXNIP	Thioredoxin interacting protein	1021.076111
103910	MYL12B	Myosin light chain 12B	1012.033325
3854	KRT6B	Keratin 6B	1011.945374
3688	ITGB1	Integrin subunit β 1	1004.073792
3312	HSPA8	Heat shock protein family A (Hsp70) member 8	1000.302063
6288	SAA1	Serum amyloid A1	999.111145
1382	CRABP2	Cellular retinoic acid binding protein 2	986.4415283
6224	RPS20	Ribosomal protein S20	975.680481
10109	ARPC2	Actin related protein 2/3 complex subunit 2	966.9124146
1992	SERPINB1	Serpin family B member 1	952.090332
306	ANXA3	Annexin A3	951.5344238
4501	MT1X	Metallothionein 1X	939.5453491
5660	PSAP	Prosaposin	936.7683105
6286	S100P	S100 calcium binding protein P	924.9679565
567	B2M	β -2-microglobulin	919.1690674
3914	LAMB3	Laminin subunit β 3	918.9204102
1308	COL17A1	Collagen type XVII α 1 chain	916.5231323
824	CAPN2	Calpain 2	912.717041
2706	GJB2	Gap junction protein β 2	904.8463745
3860	KRT13	Keratin 13	894.9153442
3646	EIF3E	Eukaryotic translation initiation factor 3 subunit E	893.5683594
5479	PPIB	Peptidylprolyl isomerase B	883.137207
7316	UBC	Ubiquitin C	875.6885986
3326	HSP90AB1	Heat shock protein 90 α family class B member 1	871.9744263
642587	MIR205HG	MIR205 host gene	864.2874146
468	ATF4	Activating transcription factor 4	850.9224243
140576	S100A16	S100 calcium binding protein A16	849.9338989
6155	RPL27	Ribosomal protein L27	841.65802

Table II. Continued.

Entrez gene ID	Gene symbol	Description	TPM
6228	RPS23	Ribosomal protein S23	837.4863281
25984	KRT23	Keratin 23	837.0656738
54541	DDIT4	DNA damage inducible transcript 4	831.8173218
112694756	LOC112694756	Uncharacterized LOC112694756	831.1845093
9349	RPL23	Ribosomal protein L23	826.6482544
7184	HSP90B1	Heat shock protein 90 β family member 1	826.4506836
1337	COX6A1	Cytochrome c oxidase subunit 6A1	820.6051025
1974	EIF4A2	Eukaryotic translation initiation factor 4A2	800.7364502
6188	RPS3	Ribosomal protein S3	796.1228638
6157	RPL27A	Ribosomal protein L27a	790.3303833
5757	PTMA	Prothymosin α	790.0863037
826	CAPNS1	Calpain small subunit 1	783.6133423
5328	PLAU	Plasminogen activator, urokinase	780.4100342
2023	ENO1	Enolase 1	778.8522949
1509	CTSD	Cathepsin D	771.4251709
10476	ATP5PD	ATP synthase peripheral stalk subunit d	768.3088989
7534	YWHAZ	Tyrosine 3-monooxygenase/tryptophan 5-monooxygenase activation protein ζ	767.7701416
292	SLC25A5	Solute carrier family 25 member 5	758.4469604
5216	PFN1	Profilin 1	753.312439
1340	COX6B1	Cytochrome c oxidase subunit 6B1	751.3442383
8407	TAGLN2	Transgelin 2	741.7597046
689	BTF3	Basic transcription factor 3	738.1211548
374	AREG	Amphiregulin	735.1116333
10376	TUBA1B	Tubulin α 1b	732.8063965
6210	RPS15A	Ribosomal protein s15a	728.9209595
3909	LAMA3	Laminin subunit α 3	723.6885986
7086	TKT	Transketolase	713.4926147
5650	KLK7	Kallikrein related peptidase 7	708.7366333
4323	MMP14	Matrix metalloproteinase 14	702.4146118
4312	MMP1	Matrix metalloproteinase 1	700.8983154
6229	RPS24	Ribosomal protein S24	700.0944824
10653	SPINT2	Serine peptidase inhibitor, Kunitz type 2	695.8338623
4831	NME2	NME/NM23 nucleoside diphosphate kinase 2	694.8643799
10971	YWHAQ	Tyrosine 3-monooxygenase/tryptophan 5-monooxygenase activation protein τ	692.3873291
5478	PPIA	Peptidylprolyl isomerase A	682.8765869
7980	TFPI2	Tissue factor pathway inhibitor 2	679.0671997
6146	RPL22	Ribosomal protein L22	678.4135132
3945	LDHB	Lactate dehydrogenase B	671.2799683
351	APP	Amyloid β precursor protein	665.9901733
1508	CTSB	Cathepsin B	665.0159302
10209	EIF1	Eukaryotic translation initiation factor 1	664.9918213
8673	VAMP8	Vesicle associated membrane protein 8	659.6922607
7416	VDAC1	Voltage dependent anion channel 1	659.1289063
4946	OAZ1	Ornithine decarboxylase antizyme 1	656.2600098
6168	RPL37A	Ribosomal protein L37a	649.401123

TPM, transcript per million.

These observations suggest an overall role for EGFR in the pathogenesis of MEC and the EGFR pathway could be a possible therapeutic target. As several drugs target this pathway, AREG-EGFR signaling was analyzed in the HCM-MEC010 cell line in the present study. The HCM-MEC010 cell line was found to express AREG and phosphorylate EGFR. Immunofluorescence analysis localized EGFR expression to the HCM-MEC010 cell membrane. These data suggest that the EGFR ligand, AREG, activated EGFR in an autocrine manner; therefore, antibodies that block AREG-EGFR binding or drugs that interfere with EGFR activation could be used for *CRTC1-MAML2* fusion-positive MEC treatment. However, further analysis is required to identify suitable therapies.

MECs are composed of mucin-producing, epidermoid, and intermediate cells; however, RNA-Seq analysis of the HCM-MEC010 cell line detected little expression of *MUC* genes in the mucous cell marker family, indicating that mucin-producing cells and intermediate cells may have been removed during culture. MECs develop in excretory duct cells (43) and the mixture of three different cell types in MECs predicts their common origin. Duct and acinar cell differentiation are typically lineage-restricted; however, after irradiation, both duct and acinar cells can differentiate into different cell types (44). It is conceivable that established epidermoid-like cells are competent to differentiate into acinar cells, which is a predicted characteristic of injured duct stem cells. Further analysis will assist in the clarification into the origin of MECs. Cancer stem cells have been hypothesized to be involved in tumor formation (43). The results of the present study potentially indicate these cells may be of the same origin.

In conclusion, a MEC cell line, HCM-MEC010, with a *CRTC1-MAML2* gene fusion was established. This cell line showed typical MEC characteristics, including AREG expression and EGFR activation; therefore, it could be used to assist in the identification of EGFR-targeted drugs for the treatment of *CRTC1-MAML2* fusion gene-harboring MEC.

Acknowledgements

The authors would like to thank Ms. Shinobu Osawa (Department of Oral and Maxillofacial Surgery, Hyogo College of Medicine, Nishinomiya, Japan) for preparation of the experiments and Ms. Takako Nanba (Department of Oral and Maxillofacial Surgery, Hyogo College of Medicine, Nishinomiya, Japan) for the management of the grants. The authors would also like to thank Nikki March and Sarah Williams for editing a draft version of the manuscript.

Funding

This study was supported by JSPS Grants-in-Aid for Scientific Research (grant nos. 16H11737 and 19H 10277), a Grant-in-Aid for Graduate Students, and a Hyogo College of Medicine and Hyogo Health Foundation Cancer Research Award.

Availability of data and materials

The datasets generated and/or analyzed during the current study are not publicly available due to a pending patent

application, but are available from the corresponding author on reasonable request.

Authors' contributions

KN, SK, KaY, KT, HK and YN conceived and designed the present study. KN, SK, KaY, YF, KyY and YN performed the experiments. KN, SK, KoY and YN analyzed the data. KN, SK and YN wrote, reviewed, and revised the manuscript. All authors read and approved the final manuscript. KN and SK confirm the authenticity of all the raw data.

Ethics approval and consent to participate

The current study was approved by the Institutional Review Board of Hyogo College of Medicine (Hyogo, Japan) and was conducted in accordance with the Declaration of Helsinki. The patient provided written informed consent to participate.

Patient consent for publication

The patient provided written informed consent for the publication of their case study.

Competing interests

The authors declare that they have no competing interests.

References

1. Sentani K, Ogawa I, Ozawa K, Sadakane A, Utada M, Tsuya T, Kajihara H, Yonehara S, Takeshima Y and Yasui W: Characteristics of 5015 salivary gland neoplasms registered in the Hiroshima tumor tissue registry over a period of 39 years. *J Clin Med* 8: 566, 2019.
2. Behboudi A, Enlund F, Winnes M, Andrén Y, Nordkvist A, Leivo I, Flaberg E, Szekely L, Mäkitie A, Grenman R, *et al*: Molecular classification of mucoepidermoid carcinomas-prognostic significance of the *MECT1-MAML2* fusion oncogene. *Genes Chromosomes Cancer* 45: 470-481, 2006.
3. Ettl T, Schwarz-Furlan S, Gosau M and Reichert TE: Salivary gland carcinomas. *Oral Maxillofac Surg* 16: 267-283, 2012.
4. Katabi N, Ghossein R, Ali S, Dogan S, Klimstra D and Ganly I: Prognostic features in mucoepidermoid carcinoma of major salivary glands with emphasis on tumour histologic grading. *Histopathology* 65: 793-804, 2014.
5. El-Naggar AK, Lovell M, Killary AM, Clayman GL and Batsakis JG: A mucoepidermoid carcinoma of minor salivary gland with t(11;19)(q21;p13.1) as the only karyotypic abnormality. *Cancer Genet Cytogenet* 87: 29-33, 1996.
6. Saade RE, Bell D, Garcia J, Roberts D and Weber R: Role of *CRTC1/MAML2* translocation in the prognosis and clinical outcomes of mucoepidermoid carcinoma. *JAMA Otolaryngol Head Neck Surg* 142: 234-240, 2016.
7. Bell D and El-Naggar AK: Molecular heterogeneity in mucoepidermoid carcinoma: Conceptual and practical implications. *Head Neck Pathol* 7: 23-27, 2013.
8. Jee KJ, Persson M, Heikinheimo K, Passador-Santos F, Aro K, Knuutila S, Odell EW, Mäkitie A, Sundelin K, Stenman G and Leivo I: Genomic profiles and *CRTC1-MAML2* fusion distinguish different subtypes of mucoepidermoid carcinoma. *Mod Pathol* 26: 213-222, 2013.
9. O'Neill ID: t(11;19) translocation and *CRTC1-MAML2* fusion oncogene in mucoepidermoid carcinoma. *Oral Oncol* 45: 2-9, 2009.
10. Seethala RR, Dacic S, Cieply K, Kelly LM and Nikiforova MN: A reappraisal of the *MECT1/MAML2* translocation in salivary mucoepidermoid carcinomas. *Am J Surg Pathol* 34: 1106-1121, 2010.

11. Tonon G, Modi S, Wu L, Kubo A, Coxon AB, Komiya T, O'Neil K, Stover K, El-Naggar A, Griffin JD, *et al*: t(11;19) (q21;p13) translocation in mucoepidermoid carcinoma creates a novel fusion product that disrupts a Notch signaling pathway. *Nat Genet* 33: 208-213, 2003.
12. Enlund F, Behboudi A, Andr  n Y, Oberg C, Lendahl U, Mark J and Stenman G: Altered Notch signaling resulting from expression of a WAMTP1-MAML2 gene fusion in mucoepidermoid carcinomas and benign Warthin's tumors. *Exp Cell Res* 292: 21-28, 2004.
13. Wu L, Liu J, Gao P, Nakamura M, Cao Y, Shen H and Griffin JD: Transforming activity of MECT1-MAML2 fusion oncoprotein is mediated by constitutive CREB activation. *EMBO J* 24: 2391-2402, 2005.
14. Coxon A, Rozenblum E, Park YS, Joshi N, Tsurutani J, Dennis PA, Kisch IR and Kaye FJ: Mect1-Maml2 fusion oncogene linked to the aberrant activation of cyclic AMP/CREB regulated genes. *Cancer Res* 65: 7137-7144, 2005.
15. Fehr A, R  ser K, Heidorn K, Hallas C, L  ning T and Bullerdiek J: A new type of MAML2 fusion in mucoepidermoid carcinoma. *Genes Chromosomes Cancer* 47: 203-206, 2008.
16. Okabe M, Miyabe S, Nagatsuka H, Terada A, Hanai N, Yokoi M, Shimozato K, Eimoto T, Nakamura S, Nagai N, *et al*: MECT1-MAML2 fusion transcript defines a favorable subset of mucoepidermoid carcinoma. *Clin Cancer Res* 12: 3902-3907, 2006.
17. Nakayama T, Miyabe S, Okabe M, Sakuma H, Ijichi K, Hasegawa Y, Nagatsuka H, Shimozato K and Inagaki H: Clinicopathological significance of the CRTC3-MAML2 fusion transcript in mucoepidermoid carcinoma. *Mod Pathol* 22: 1575-1581, 2009.
18. Chen Z, Chen J, Gu Y, Hu C, Li JL, Lin S, Shen H, Cao C, Gao R, Li J, *et al*: Aberrantly activated AREG-EGFR signaling is required for the growth and survival of CRTC1-MAML2 fusion-positive mucoepidermoid carcinoma cells. *Oncogene* 33: 3869-3877, 2014.
19. Dahse R, Driemel O, Schwartz S, Dahse J, Kromeyer-Hauschild K, Berndt A and Kosmehl H: Epidermal growth factor receptor kinase domain mutations are rare in salivary gland carcinomas. *Br J Cancer* 100: 623-625, 2009.
20. Nakano T, Yamamoto H, Hashimoto K, Tamiya S, Shiratsuchi H, Nakashima T, Nishiyama K, Higaki Y, Komune S and Oda Y: HER2 and EGFR gene copy number alterations are predominant in high-grade salivary mucoepidermoid carcinoma irrespective of MAML2 fusion status. *Histopathology* 63: 378-392, 2013.
21. Warner KA, Adams A, Bernardi L, Nor C, Finkel KA, Zhang Z, McLean SA, Helman J, Wolf GT, Divi V, *et al*: Characterization of tumorigenic cell lines from the recurrence and lymph node metastasis of a human salivary mucoepidermoid carcinoma. *Oral Onco* 49: 1059-1066, 2013.
22. Liu X, Ory V, Chapman S, Yuan H, Albanese C, Kallakury B, Timofeeva OA, Nealon C, Dakic A, Simic V, *et al*: ROCK inhibitor and feeder cells induce the conditional reprogramming of epithelial cells. *Am J Pathol* 180: 599-607, 2012.
23. Dulbecco R and Vogt M: Plaque formation and isolation of pure lines with poliomyelitis viruses. *J Exp Med* 99: 167-182, 1954.
24. Noguchi K, Wakai K, Kiyono T, Kawabe M, Yoshikawa K, Hashimoto-Tamaoki T, Kishimoto H and Nakano Y: Molecular analysis of keratocystic odontogenic tumor cell lines derived from sporadic and basal cell nevus syndrome patients. *Int J Oncol* 51: 1731-1738, 2017.
25. Hiromoto T, Noguchi K, Yamamura M, Zushi Y, Segawa E, Takaoka K, Moridera K, Kishimoto H and Urade M: Up-regulation of neutrophil gelatinase-associated lipocalin in oral squamous cell carcinoma: Relation to cell differentiation. *Oncol Rep* 26: 1415-1421, 2011.
26. Gupta R, Kalita P, Patil O and Mohanty S: An investigation of folic acid-protein association sites and the effect of this association on folic acid self-assembly. *J Mol Model* 21: 308, 2015.
27. Rio DC, Ares M Jr, Hannon GJ and Nilsen TW: Purification of RNA using TRIzol (TRI reagent). *Cold Spring Harb Protoc* 2010: pdb.prot5439, 2010.
28. Prophet EB, Mills B, Arrington JB and Sobin LH: Laboratory methods in histotechnology (Armed Forces Institute of Pathology). American Registry of Pathology, Washington, DC, 1992.
29. Seethala RR: An update on grading of salivary gland carcinomas. *Head Neck Pathol* 3: 69-77, 2009.
30. Ohnishi Y, Minamino Y, Kakudo K and Nozaki M: Resistance of oral squamous cell carcinoma cells to cetuximab is associated with EGFR insensitivity and enhanced stem cell-like potency. *Oncol Rep* 32: 780-786, 2014.
31. Meng C, Wang S, Wang X, Lv J, Zeng W, Chang R, Li Q and Wang X: Amphiregulin inhibits TNF-  induced alveolar epithelial cell death through EGFR signaling pathway. *Biomed Pharmacother* 125: 109995, 2020.
32. Telesco SE, Vadigepalli R and Radhakrishnan R: Molecular modeling of ErbB4/HER4 kinase in the context of the HER4 signaling network helps rationalize the effects of clinically identified HER4 somatic mutations on the cell phenotype. *Biotechnol J* 8: 1452-1464, 2013.
33. Li X, Huang Q, Wang S, Huang Z, Yu F and Lin J: HER4 promotes the growth and metastasis of osteosarcoma via the PI3K/AKT pathway. *Acta Biochim Biophys Sin (Shanghai)* 52: 345-362, 2020.
34. Luna MA: Salivary mucoepidermoid carcinoma: Revisited. *Adv Anat Pathol* 13: 293-307, 2006.
35. Mitra A, Mishra L and Li S: Technologies for deriving primary tumor cells for use in personalized cancer therapy. *Trends Biotechnol* 31: 347-354, 2013.
36. Okumura Y, Miyabe S, Nakayama T, Fujiyoshi Y, Hattori H, Shimozato K and Inagaki H: Impact of CRTC1/3-MAML2 fusions on histological classification and prognosis of mucoepidermoid carcinoma. *Histopathology* 59: 90-97, 2011.
37. Tirado Y, Williams MD, Hanna EY, Kaye FJ, Batsakis JG and El-Naggar AK: CRTC1/MAML2 fusion transcript in high grade mucoepidermoid carcinomas of salivary and thyroid glands and Warthin's tumors: Implications for histogenesis and biologic behavior. *Genes Chromosomes Cancer* 46: 708-715, 2007.
38. Anzick SL, Chen WD, Park Y, Meltzer P, Bell D, El-Naggar AK and Kaye FJ: Unfavorable prognosis of CRTC1-MAML2 positive mucoepidermoid tumors with CDKN2A deletions. *Genes Chromosomes Cancer* 49: 59-69, 2010.
39. Komiya T, Park Y, Modi S, Coxon AB, Oh H and Kaye FJ: Sustained expression of Mect1-Maml2 is essential for tumor cell growth in salivary gland cancers carrying the t(11;19) translocation. *Oncogene* 25: 6128-6132, 2006.
40. Wu J, Wang N, Yang Y, Jiang G, Zhan H and Li F: LINC01152 upregulates MAML2 expression to modulate the progression of glioblastoma multiforme via Notch signaling pathway. *Cell Death Dis* 12: 115, 2021.
41. Amelio AL, Fallahi M, Schaub FX, Zhang M, Lawani MB, Alperstein AS, Southern MR, Young BM, Wu L, Zajac-Kaye M, *et al*: CRTC1/MAML2 gain-of-function interactions with MYC create a gene signature predictive of cancers with CREB-MYC involvement. *Proc Natl Acad Sci USA* 111: 3260-3268, 2014.
42. Shinomiya H, Ito Y, Kubo M, Yonezawa K, Otsuki N, Iwae S, Inagaki H and Nibu KI: Expression of amphiregulin in mucoepidermoid carcinoma of the major salivary glands: A molecular and clinicopathological study. *Hum Pathol* 57: 37-44, 2016.
43. Porcheri C and Mitsiadis TA: Physiology, pathology and regeneration of salivary glands. *Cells* 8: 976, 2019.
44. Weng PL, Aure MH, Maruyama T and Ovitt CE: Limited regeneration of adult salivary glands after severe injury involves cellular plasticity. *Cell Rep* 24: 1464-1470.e3, 2018.



This work is licensed under a Creative Commons Attribution-NonCommercial-NoDerivatives 4.0 International (CC BY-NC-ND 4.0) License.